Cancer Genes and Genomics

Molecular Cancer Research

Overexpression of miR-21 Promotes an *In vitro* Metastatic Phenotype by Targeting the Tumor Suppressor RHOB

Erin C. Connolly[1,2], Koenraad Van Doorslaer[2], Leslie E. Rogler[1], and Charles E. Rogler[1,2]

Abstract

Metastasis is a multistep process that involves the deregulation of oncogenes and tumor suppressors beyond changes required for primary tumor formation. RHOB is known to have tumor suppressor activity, and its knockdown is associated with more aggressive tumors as well as changes in cell shape, migration, and adhesion. This study shows that oncogenic microRNA, miR-21, represses RHOB expression by directly targeting the 3′ untranslated region. Loss of miR-21 is associated with an elevation of RHOB in hepatocellular carcinoma cell lines Huh-7 and HepG2 and in the metastatic breast cancer cell line MDA-MB-231. Using *in vitro* models of distinct stages of metastasis, we showed that loss of miR-21 also causes a reduction in migration, invasion, and cell elongation. The reduction in migration and cell elongation can be mimicked by overexpression of RHOB. Furthermore, changes in miR-21 expression lead to alterations in matrix metalloproteinase-9 activity. Therefore, we conclude that miR-21 promotes multiple components of the metastatic phenotype *in vitro* by regulating several important tumor suppressors, including RHOB. *Mol Cancer Res; 8(5); 691–700. ©2010 AACR.*

Introduction

Primary hepatocellular carcinoma (HCC) is among the most frequent and aggressive malignancies in the world. It is especially common in Southeast Asian populations where infection with hepatitis B and C virus is prevalent (1). Although there have been advances in diagnostic modalities that improve the rate of detection, the long-term survival of HCC patients is poor due to the high incidence of recurrence after initial treatment (2). Genetic and pathologic studies show that recurrence of HCC is split into two types: multicentric development of new tumors and intrahepatic metastasis of the original HCC (3). Intrahepatic metastasis occurs during late-stage HCC and is thought to develop through tumor cell dispersal via the portal vein (4).

Metastasis is a multistep process consisting of cell detachment from the primary tumor, extravasation, and finally invasion of the secondary site. Recently, several small regulatory noncoding RNA molecules, known as microRNAs (miRNA), have been shown to function as tumor suppressors or oncogenes and have been linked to invasion (5). miRNAs act to repress gene expression on the posttranscriptional level through mechanisms involving either degradation or translational repression of their target mRNAs (6-8). Gabriely et al. (9) showed that miR-21 promotes glioma migration and invasion through targeting of matrix metalloproteinase (MMP) inhibitors. Additionally, knockdown of miR-21 expression in glioma cell lines leads to a decrease in migration, which was hypothesized to be due to miR-21 directly targeting the metalloproteinase inhibitor RECK (reversion-inducing cysteine-rich protein with Kazal motifs; ref. 10).

We previously showed that miR-21 is overexpressed in both primary HCC (11) and HCC cell lines (12). Increased miR-21 expression has also been reported in a wide range of tumor types (6, 12-14). Its overexpression has been linked to inhibition of apoptosis and promotion of cell proliferation (11, 14-16). Zhu et al. (10) showed that knockdown of miR-21 in MDA-MB-231 cells led to a decrease in the formation of tumors in the lung after tail vein injection.

In this study, we identify the tumor suppressor gene *RHOB* (ras homolog gene family, member B) as a target of miR-21. RHOB is a small GTPase known to regulate actin organization and vesicle transport. In contrast to its family members RHOA and RHOC, RHOB overexpression inhibits tumor formation (17). Overexpression of RHOA has been linked to HCC metastasis (18). However, a role for RHOB in metastatic phenotype of HCC has not been previously reported. In this report, we show that RHOB expression is modulated by the oncomiR miR-21. Additionally, we show that the miR-21–induced loss of RHOB expression contributes to the promotion of several *in vitro* cell phenotypes associated with increased metastatic potential of cells.

Authors' Affiliations: [1]Marion Bessin Liver Research Center, Division of Hepatology, Department of Medicine and [2]Department of Microbiology and Immunology, Albert Einstein College of Medicine, Bronx, New York

Note: Supplementary data for this article are available at Molecular Cancer Research Online (http://mcr.aacrjournals.org/).

Corresponding Author: Charles E. Rogler, Marion Bessin Liver Research Center, Division of Hepatology, Department of Medicine, and Department of Microbiology and Immunology, Albert Einstein College of Medicine, 1300 Morris Park Avenue, Bronx, NY 10461. Phone: 718-430-2607; Fax: 718-430-8975. E-mail: crogler@aecom.yu.edu

doi: 10.1158/1541-7786.MCR-09-0465

Materials and Methods

Cell culture and oligonucleotide transfections. The Huh-7 and HepG2 HCC cell lines and MDA-MB-231 breast cancer cell line (which express high levels of miR-21; refs. 11-13) were maintained in DMEM supplemented with 10% fetal bovine serum, sodium, pyruvate, nonessential amino acids, and penicillin-streptomycin. miR-21 inhibition was achieved by transfecting cells with 100 nmol/well of 2′-*O*-methyl antisense oligonucleotides (ASO; IDT) by Lipofectamine RNAiMAX (Invitrogen) according to the manufacturer's protocol. 2′-*O*-methyl ASO sequences were as follows: 5′-AUCGAAUAGUCUGACUACAACU-′3 (miR-21 ASO) and 5′-CCCCCCCCCCCCCCCCCCCC-′3 (negative ASO). Overexpression of miR-21 was achieved by transfecting cells with synthetic RNA duplex (mimic; Dharmacon) at 10 nmol/well corresponding to the mature miR-21 and negative control (cel-miR-67). HepG2 cells were plated on poly-D-lysine–coated tissue culture plates (Becton Dickinson) to increase transfection efficiency.

Quantitative reverse transcription-PCR analysis of mRNA and miRNA expression. RNA was isolated from cells 48 hours after transfection using the RNAqueous RNA isolation kit (Ambion). Normal liver RNA was obtained from Ambion. cDNA was produced using the High Capacity cDNA Reverse Transcription kit (Applied Biosystems). Taqman probes (RHOB, RECK, PTEN, PDCD4, and B2M) were used (Applied Biosystems), and quantitative reverse transcription-PCR (qRT-PCR) was done in accordance with the manufacturer's protocols. B2M was used as the reference gene for normalization. miR-21 expression levels were quantified using Taqman MicroRNA Assay kit (Applied Biosystems). Taqman and cDNA kits (Applied Biosystems) were used to prepare all samples for qRT-PCR, in accordance with the manufacturer's instructions. RNU43 was used as a reference. qRT-PCR analysis was done using an ABI 7000 real-time detection system. Expression levels were compared with either normal liver or cell lines mock transfected with Lipofectamine only (consisted no treatment) using the $2^{-\Delta\Delta Ct}$ method. Significance was determined using paired *t* test of the ΔC_t values ($P < 0.05$).

Expression vector and siRNA. Cells were transfected with a set of three siRNA duplexes (IDT) per gene at 10 nmol/well, with Lipofectamine 2000 (Invitrogen), according to the manufacturer's protocol. The level of knockdown was determined by qRT-PCR (Table 1).

The overexpression vector pQE-T7 containing the RHOB protein coding sequence was purchased from Qiagen. Cells were transfected with either 10 ng/well of the RHOB construct or empty pQE-T7 vector using Lipofectamine 2000. The level of overexpression was determined by qRT-PCR.

Western blot. Cells were lysed in radioimmunoprecipitation assay buffer (Sigma) containing protease inhibitors (Roche Diagnostic). Protein (40 μg) was loaded on 10% Tris-glycine gels (Invitrogen) and transferred onto polyvinylidene difluoride membrane (Invitrogen). Blots were probed with antibodies (Cell Signaling) to RHOB and COX IV (loading control) and visualized by chemiluminescence reagent (PerkinElmer Life Science). NIH ImageJ was used to determine the pixel intensity of each band. Relative expression was determined by dividing the pixel intensity of the sample by that of the loading control. The average of three blots was presented.

Reporter assay. Three 3′ untranslated region (UTR) fragments were cloned immediately downstream of the *Renilla* luciferase gene in a *Renilla*/firefly luciferase reporter plasmid, psiCHECK-2 (Promega). The cloned fragments were (*a*) full 3′UTR (the complete RHOB 3′UTR), (*b*) nucleotides 1326 to 1332 (the complete predicted miR-21 target site of the RHOB 3′UTR), and (*c*) mutated nucleotides 1326 to 1332 (the full predicted miR-21RHOB 3′ UTR target site with complete mutation of the seed region). The 3′UTR of RHOB was amplified with primers that carried *Xho*I/*Not*I endonuclease sites. Oligonucleotides for the nucleotides 1326 to 1332 and mutated nucleotides 1326 to 1332 with *Xho*I/*Not*I endonuclease sites were obtained from IDT (Table 2).

Huh-7 cells were transfected at ~30% confluence with 25 ng reporter construct per well plus or minus inhibitor/mimic miRNA (0.25 pmol/L/well) using Lipofectamine 2000 according to the manufacturer's protocol. Twenty-four hours after transfection, the cells were lysed and *Renilla* luciferase activity was measured by the Dual Luciferase Reporter Assay (Promega) on a BMG FLUOstar Optima plate reader in accordance with the manufacturer's protocol. Firefly luciferase signal was used for transfection efficacy. The *Renilla*/firefly luiferase ratio for each experimental

Table 1. Negative control: IDT DS scramble negative siRNA

siRNA	Duplex		
Negative control	1	5′-CUUCCUCUCUUUCUCUCCCUUGUGA-3′	5′-UCACAAGGGAGAGAAAGAGAGGAAGGA-3′
RHOB	1	5′-GGCAUUCUCUAAAGCUAUGUGAAAT-3′	5′-AUUUCACAUAGCUUUAGAGAAUGCCUU-3′
	2	5′-AGCAAGAUGGUGUUAUUUAAGGT-3′	5′-ACCCUUAAAUAACACCAUCUUAGCUCC-3′
	3	5′-ACCUCUGUACCAGAGAAUACACCUGC-3′	5′-GCAGGUGUAUUCUCUGUACAGAGGUGC-3′
RECK	1	5′-ACAAUGUAGAUAAGUGUUCUGUCUG-3′	5′-CAGACAGAACACUUAUCUACAUUGUGC-3′
	2	5′-AGAUUAACCUUGUCAUAGUAAAUC-3′	5′-GAUUUACUAUGACAAGGUUUAAUCUGC-3′
	3	5′-GCAUGUUGUCUAAGAAAUUGAAUAC-3′	5′-GUAUUCAAUUUCUUAGACAACAUGCAU-3′

Table 2. Primers and oligos

Fragment	Forward	Reverse
Full 3′UTR	5′-GTACCTCGAGTTTGTGCCTGTCCTAGAAT	5′-CAGTACGCGGCCGCAATGTCATCATCATAGTCTTTAAT
Nucleotides	5′-GTACCTCGAGACAATGACAAA	5′-GTACCTCGAGACAATGACAAAATGGTGAGCTTA
1326-1332	5′-ATGGTGAGCTTATGATGTTTACATAAAAGT TCTATAAGCTGTGTATACAGTTTTCAGTAC GCGGCGC	5′-TGATGTTTACATAAAAGTTCTATAAGCTGTGTA 5′-TACAGTTTTCAGTACGCGGCGC
Mutated	5′-GTACCTCGAGACAATGACAAAATGGTGA	5′-GTACCTCGAGACAATGACAAAATGGTGAGCTTAT
nucleotides	5′-GCTTATGATGTTTACATAAAAGTTCTGCCGA	5′-GATGTTTACATAAAAGTTCTGCCGATGTTGTAT
1326-1332	5′-TGTTGTATACAGTTTTCAGTACGCGGCGC	5′-ACAGTTTTCAGTACGCGGCGC

plasmid treated with inhibitor/mimic miRNA was normalized to no treatment of that plasmid.

Migration assay. Cells were transfected with either inhibitor/mimic miRNA, siRNA, or expression vectors. Additionally, in select experiments, cells were treated with mitomycin C (5 μg/mL). The confluent monolayer was scratched 24 hours after transfection to create a clear area within the monolayer or wound. The wound was

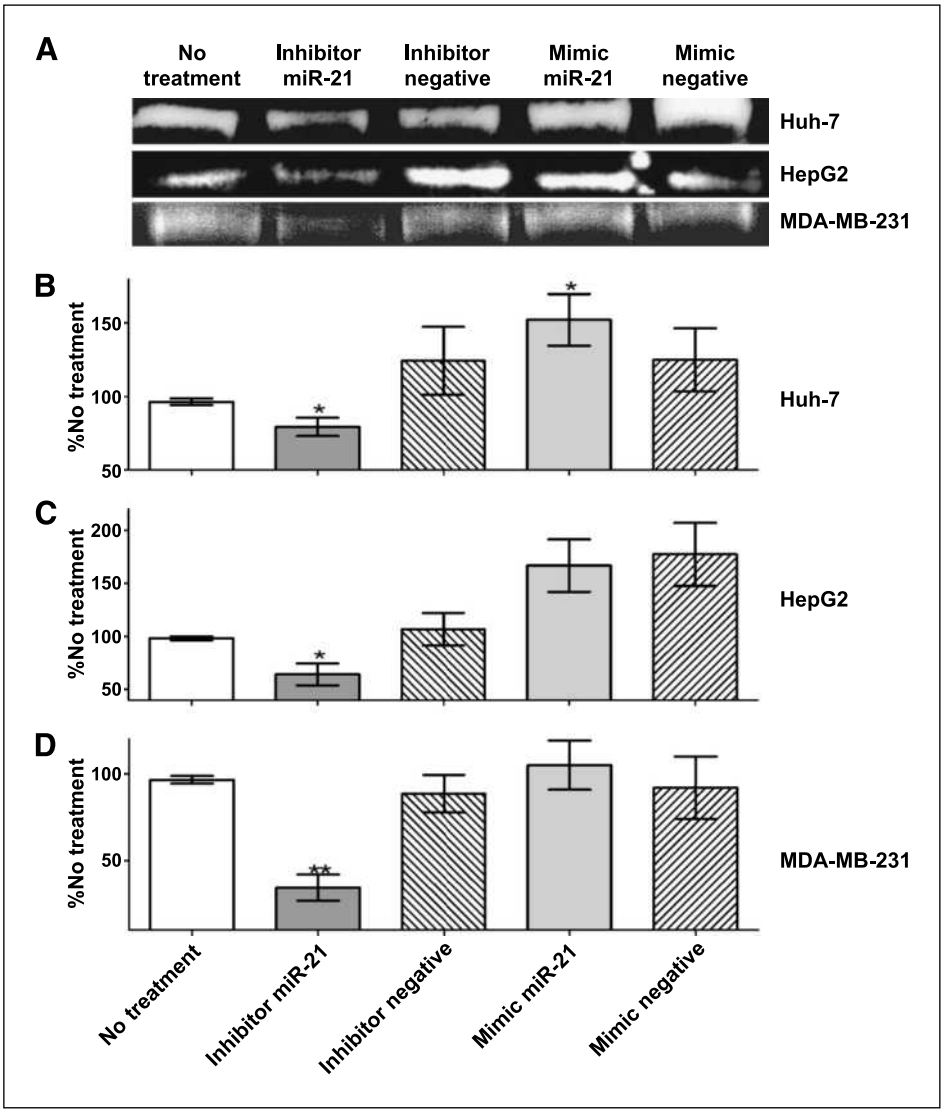

FIGURE 1. A, representative results from zymography. Cells were transfected with inhibitor/mimic miRNA and conditioned media were analyzed for MMP-9 activity by gelatin zymography. Quantification of four individual experiments per cell line Huh-7 (B), HepG2 (C), and MDA-MB-231 (D) was done using NIH ImageJ, measuring the pixel intensity of each band. Data are expressed as % no treatment (Lipofectamine only). *, $P < 0.05$; **, $P < 0.001$; ***, $P < 0.0001$.

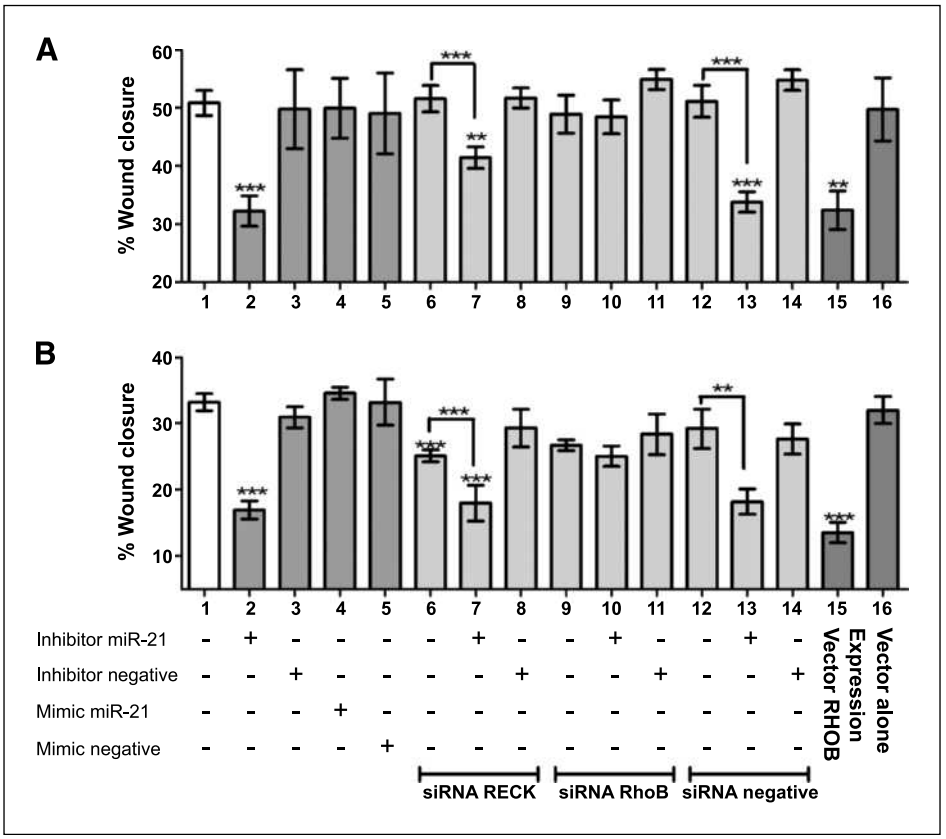

FIGURE 2. Results of migration assay done on cells transfected with either inhibitor/mimic miRNA, siRNA, or expression vectors. The confluent monolayer was scratched 24 h after transfection to create a wound. Quantification of four individual experiments (10 measurements per wound, 8 wounds per treatment). Data are expressed as % wound closure compared with time 0. A, Huh-7 48 h after wound. B, MDA-MB-231 cells 24 h after wound. *, $P < 0.05$; **, $P < 0.001$; ***, $P < 0.0001$.

photographed over 48 hours at 4× using a Nikon inverted phase microscope and digital camera with the Olympus DP Controller software. The width of the wound was measured using NIH ImageJ and then compared with time 0 for four independent experiments (10 measurements per wound, 8 wounds per treatment).

Zymography. Cells were transfected with inhibitor/mimic miRNA, and conditioned media were harvested after 48 hours. Conditioned media (80 μg protein) were mixed with sample buffer 1:1 (Invitrogen) and run on 10% zymogram (gelatin) gel (Invitrogen). Gels were then incubated at room temperature in zymogram renaturing buffer (Invitrogen), followed by being equilibrated in zymogram development buffer (Invitrogen) overnight at 37°C. Gels were washed and stained with Coomassie blue. Quantification of the zymography was determined using NIH ImageJ, and for each cell line, the no-treatment level of secreted MMP-9 was set at 100%.

Actin staining. Forty-eight hours after cells were transfected with inhibitor/mimic miRNA or expression vectors, cells were fixed with 4% paraformaldehyde, followed by permeabilizing with Triton X-100 and staining with Alexa Fluor 488 phalloidin (Invitrogen). The cells were imaged at 60× using a Nikon inverted phase microscope and digital camera with the Olympus DP Controller software. Cell elongation was calculated as the ratio of the longest cord through the cell to the longest axis perpendicular to it using NIH ImageJ.

Invasion assay. Cells were transfected with inhibitor/mimic miRNA or expression vector. Twenty-four hours after transfection, 1.0×10^6 cells/mL in serum-free media were placed in an invasion chamber (Chemicon) on top of extracellular matrix, with 10% fetal bovine serum as a chemoattractant. Cells were incubated in the invasion chamber for 72 hours (HCC cell lines) or 24 hours (MDA-MB-231), after which cells that did not invade the matrix and extracellular matrix were removed and the filter was stained (Coomassie blue) in accordance to the manufacturer's protocol. The stained cells were eluted from the membrane and absorbance of the sample at 560 nm was read.

Statistical analysis. Prism 5 software was used to do statistical analysis. Paired *t* test was used to determine the significance between no-treatment and experimental sets. *P* values of <0.05 were considered to be significant. The asterisks in all the figures in the article and in the Supplementary Data stand for the following levels of significance: *, $P < 0.05$; **, $P < 0.001$; ***, $P < 0.0001$. Error bars and graphs represented mean ± SEM.

Results

***Changes in miR-21 levels alter MMP-9 activity* in vitro.** Increased MMP activity has been associated with the metastatic phenotype of cancer cells, and its expression has been often used as an indicator of the metastatic potential

(19). miR-21 is not predicted to directly target MMPs. However, it has been previously reported that there are reductions in MMP-9 and MMP-2 mRNA levels after inhibition of miR-21, suggesting that the decrease in miR-21 levels may lead to a reduction of the metastatic phenotype (15, 20). Therefore, we asked whether knocking down miR-21 reduced the activity of MMP-9 in the media of tumor cells. Treatment of HepG2, Huh-7, and MDA-MB-231 cells with antisense inhibitor against miR-21 reduced miR-21 levels as judged by qRT-PCR (Supplementary Fig. S1). Concurrently, zymography of conditioned media from miR-21 inhibitor-treated cells revealed reductions of an average of 36%, 21%, and 66% in MMP-9 activity in all three cell lines, respectively (Fig. 1A-D). In a reverse approach, overexpression (using a mimic transfection) significantly increased MMP-9 secretion from Huh-7 cells and not quite significantly for HepG2 and MDA-MB-231 cells (Fig. 1A-D). This is consistent with qRT-PCR data that showed that the highest increase in miR-21 occurred in Huh-7 cells (Supplementary Figs. S1 and S2). This suggests that the increased miR-21 levels in HepG2 and MDA-MB-231 cells were not quite high enough for MMP-9 secretion to reach statistical significance.

***miR-21 promotes migration* in vitro.** An important component of the invasive profile of a cell is its ability to migrate. We hypothesized that miR-21 expression promotes migration. To determine the effect of loss of miR-21 on migration, we used an *in vitro* wound closure assay. In both HCC cell lines and MDA-MB-231 cells, miR-21 inhibitor treatment significantly reduced migration as measured by a wound closure assay (Fig. 2A and B, lane 2; Supplementary Fig. S3). This decrease was not due to effects of the inhibitor on cell growth because a similar reduction in wound closure was obtained in the presence or absence of mitomycin C, an inhibitor of cell proliferation (Supplementary Fig. S4).

miR-21 targeting of RECK is not sufficient in promoting migration. It has been proposed that miR-21 promotes migration and invasion by targeting inhibitors of MMPs, one of which is RECK (10). Increased RECK expression in endothelial and melanoma cell lines causes a reduction in cell migration, measured by the wound-healing assay (21). Therefore, we asked whether the responses we observed above could be due to the regulation of RECK. If this was the case, we predicted that siRNA knockdown of RECK should restore cell migration in cells where miR-21 was knocked down. qRT-PCR analysis of RECK expression showed a significant reduction in RECK expression in both siRNA-treated Huh-7 (−4.36-fold) and MDA-MB-231 (−7.28-fold) compared with mock-transfected cells (Supplementary Fig. S5). Knockdown of RECK, in combination with miR-21 inhibitor treatment, yielded only a partial (not significant) restoration of wound closure in Huh-7 and MDA-MB-231 cells (Fig. 2A and B, lane 2 versus lane 7). Treatment with siRNA RECK and siRNA negative control, alone or in conjunction with control inhibitor, had no effect on Huh-7 cell migration (Fig. 2A, lanes 6, 8, and 12-14). The reason that siRNA RECK alone had no effect on migration in our model is most likely due to the fact that RECK is already very low due to the constitutive high level of miR-21 in the cells.

Bioinformatic analysis of miR-21 targets identifies RHOB as a potential target. TargetScan4.1

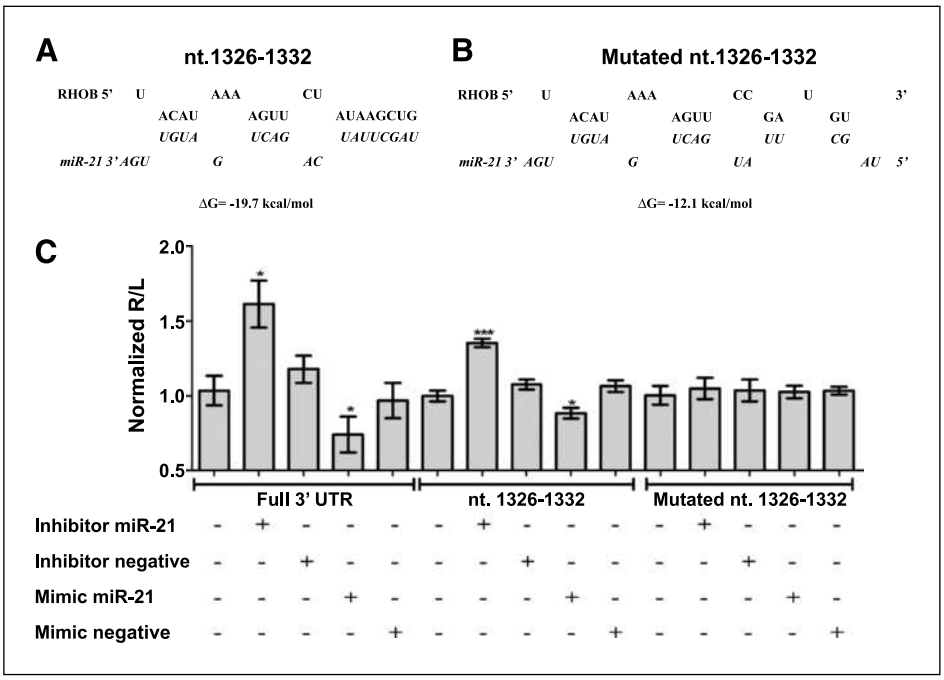

FIGURE 3. A, predicted binding hybridization of miR-21 with RHOB 3′UTR. The minimum free energy required for RNA hybridization is indicated. B, mutated miR-21 RHOB binding site. C, Dual Luciferase Reporter Assay in Huh-7 cell treated with inhibitor/mimic miRNA and three *Renilla*/firefly luciferase reporter construct: (a) full 3′UTR (the complete RHOB 3′UTR), (b) nucleotides 1326 to 1332 (the complete predicted miR-21 target site), (c) mutated nucleotides 1326 to 1332 seed region. Data presented for each construct as the normalized *Renilla*/firefly luciferase ratio (R/L). *, $P < 0.05$; **, $P < 0.001$; ***, $P < 0.0001$.

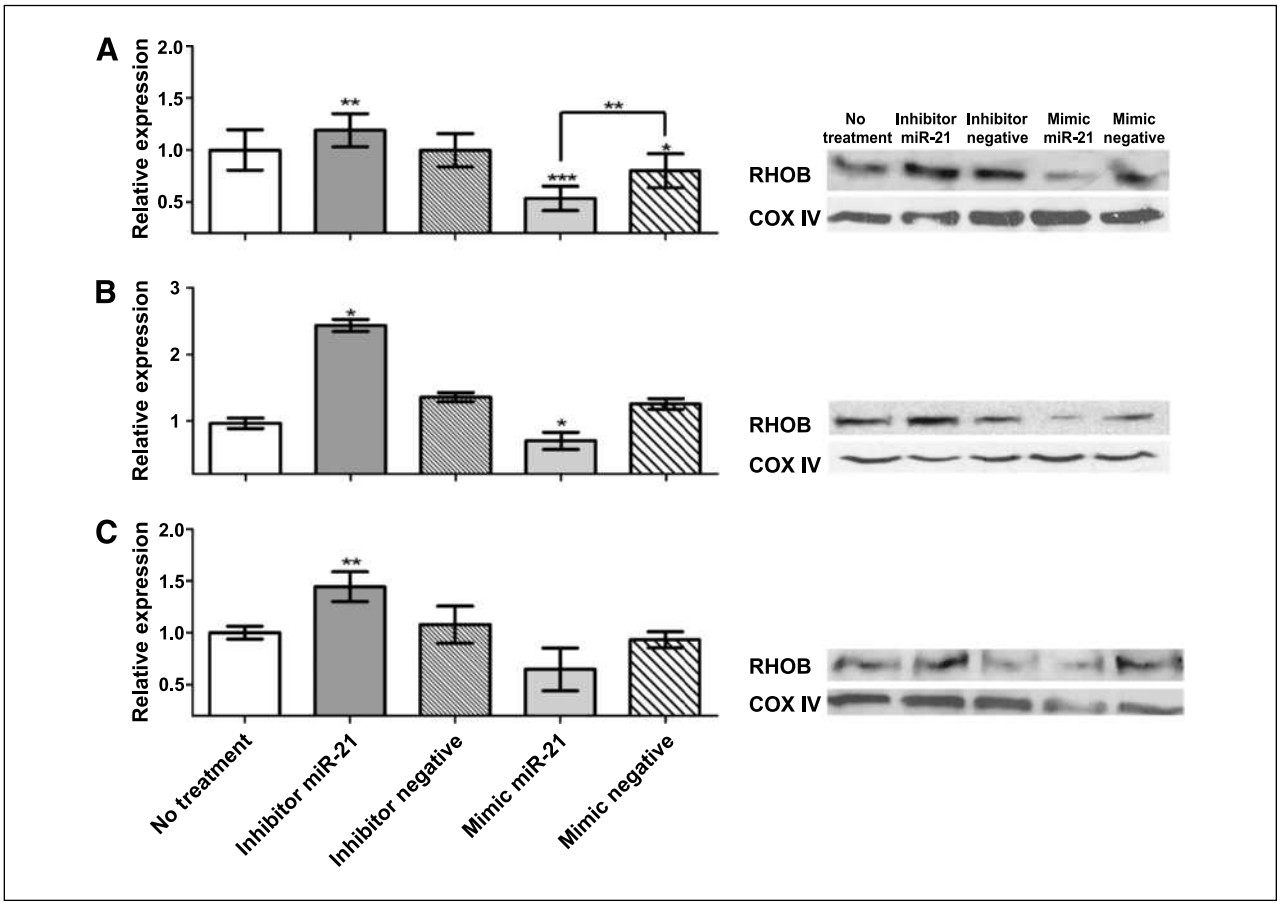

FIGURE 4. Western blot analysis of RHOB protein expression after transfection with inhibitor/mimic miRNA. Relative expression of the protein was determined by dividing the pixel intensity of the protein band by the pixel intensity of the loading control band. The average of three blots is presented. A, Huh-7 cells. B, HepG2 cells. C, MDA-MB-231 cells. *, $P < 0.05$; **, $P < 0.001$; ***, $P < 0.0001$.

(http://www.targetscan.org), a sequence miRNA target analysis software, predicted miR-21 to have 186 conserved targets. Expressed sequence tag profiles (http://www.ncbi.nlm.nih.gov/UniGene) were used to approximate gene expression patterns of predicted targets in normal liver. Predicted targets with >14 transcripts per million in normal liver were scored as expressed. Next, the targets were screened for reported tumor suppressor activity, revealing 16 targets that fell into three functional groups: invasion/migration, cell cycle/apoptosis, and cell signaling (Supplementary Table S1). Six of the 16 genes in these groups are confirmed targets of miR-21, including RECK. One of the members of invasion/migration category that had not yet been validated was RHOB. qRT-PCR analysis showed that the expression of RHOB is reduced in HCC 2-fold compared with normal liver, which was comparable with the repression of PTEN expression, a known miR-21 target (Supplementary Fig. S6; ref. 15). Additionally, loss of RHOB has been associated with increased invasion in cancer (22). In light of these observations, we hypothesized that RHOB might be one of the additional factor(s) targeted by miR-21 for the promotion of metastasis.

RHOB is directly targeted by miR-21. miR-21 has a conserved target site at nucleotides 1326 to 1332 of the RHOB 3′UTR and a TargetScan context score of 84%. The predicted hybridization of miR-21 to RHOB mRNA was determined using RNA hybrid software (Fig. 3A; ref. 23). The minimum free energy (ΔG) required for RNA hybridization is −19.7 kcal/mol. The ΔG for RNA hybridization for RECK/miR-21 is −22.7 kcal/mol.

To determine whether miR-21 is directly regulating RHOB, a reporter construct was made containing the 3′UTR of RHOB (full 3′UTR construct) mRNA immediately downstream of the *Renilla* luciferase gene in the dual luciferase reporter plasmid psiCHECK-2 (Promega). Huh-7 cells were cotransfected with the reporter plasmid alone and in the presence of either miR-21 inhibitor or mimic and assayed 24 hours after transfection. Cotransfection of the RHOB 3′UTR reporter plasmid with miR-21 inhibitor increased the *Renilla*/luciferase ratio by 60%. Conversely, cotransfection with the mimic miR-21 decreased the *Renilla*/luciferase ratio by 30% (Fig. 3C).

Two additional reporter constructs were used to determine whether the predicted target site at nucleotides

1326 to 1332 of the RHOB 3′UTR was responsible for the regulation observed in the full 3′UTR. The nucleotide 1326 to 1332 constructs exhibited a 30% increase in *Renilla*/luciferase ratio when cotransfected with miR-21 inhibitor. Cotransfection of the shorter construct with miR-21 mimic decreased the *Renilla*/luciferase ratio by 20%. Mutation of the seed sequence at the 1326 to 1332 putative target site (Fig. 3B) abolished these effects (Fig. 3C). Western blot analysis of RHOB expression revealed that knockdown of miR-21 led to an increase of 10%, 80%, and 20% in RHOB protein expression in Huh-7, HepG2, and MDA-MB-231 cells, respectively (Fig. 4A-C). It remains possible that additional nonseed-containing miR-21 sites may exist in the 3′UTR that we would not have been identified with the current experimental approach.

***Loss of RHOB expression by miR-21 promotes migration* in vitro.** If the reduction in migration observed in miR-21 inhibitor-treated cells was due to the restoration of RHOB activity, then siRNA knockdown of RHOB should restore cell migration in miR-21 inhibitor-treated cells. The expression of RHOB was significantly reduced after siRNA treatment in both Huh-7 (–2.10-fold) and MDA-MB-231 (–1.77-fold) compared with untreated cells (Supplementary Fig. S5). Huh-7 cells treated with miR-21 inhibitor had only 30% wound closure, whereas treatment with the combination of RHOB siRNA plus miR-21 inhibitor restored wound closure to 50%, showing full restoration to no-treatment levels (Fig. 2A, lane 10; Supplementary Fig. S5). Treatment with negative control siRNA had no effect on wound closure (Fig. 2A, lane 13). Similar results were obtained using the MDA-MB-231 cells (Fig. 2B).

On the other hand, transfection with a RHOB expression vector increased RHOB in both Huh-7 (2.09-fold) and MDA-MB-231 (3.57-fold) cells. This increase was comparable with mRNA RHOB level induced by miR-21 inhibitor treatment (Supplementary Fig. S7).

Elevated RHOB reduced wound closure (30% wound closure; Fig. 2A, lane 15 versus lane 16). Additionally, ectopic expression of RHOB in MDA-MB-231 cells also showed a reduction in migration (13% wound closure)

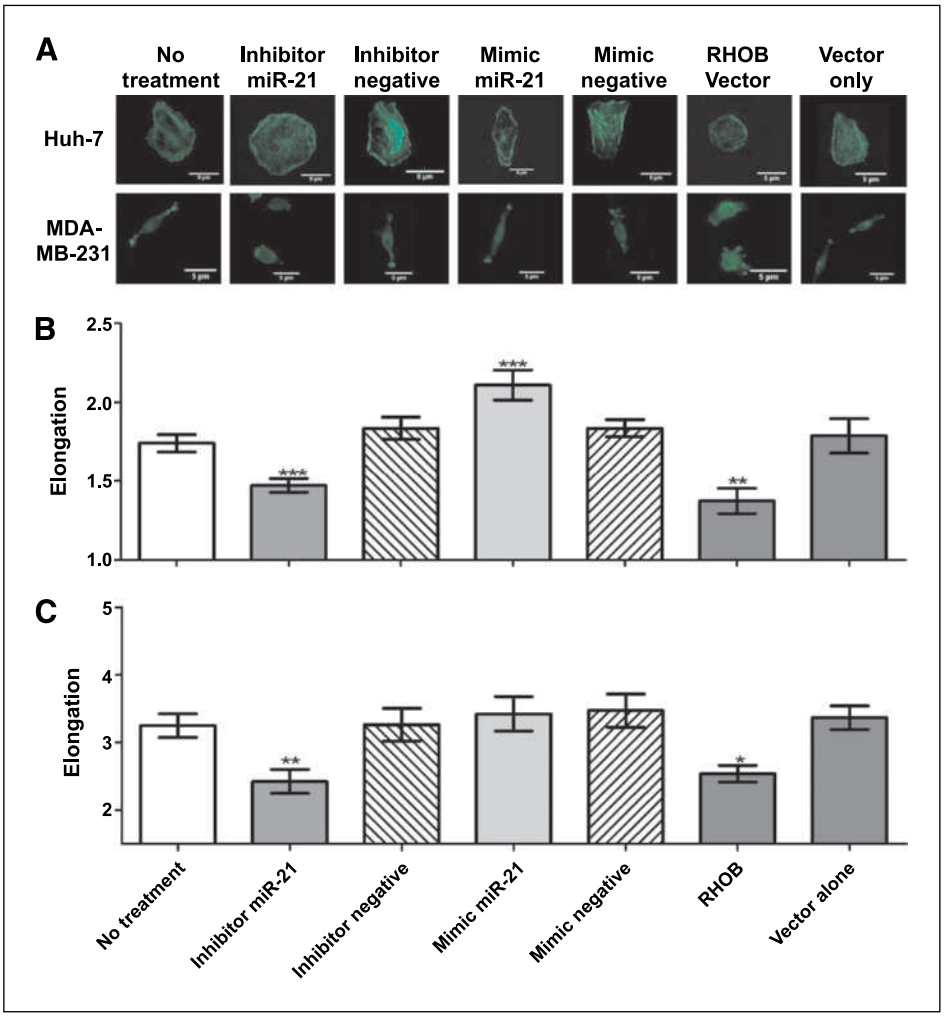

FIGURE 5. A, immnocytochemistry of actin structure with Alexa Fluor 488 phalloidin 48 h after transfection with either inhibitor/mimic miRNA or expression vector RHOB or vector alone. Quantification of cell elongation for 200 cells per cell line [Huh-7 (B) and MDA-MB-231 (C) cells] was done using NIH ImageJ. *, $P < 0.05$; **, $P < 0.001$; ***, $P < 0.0001$.

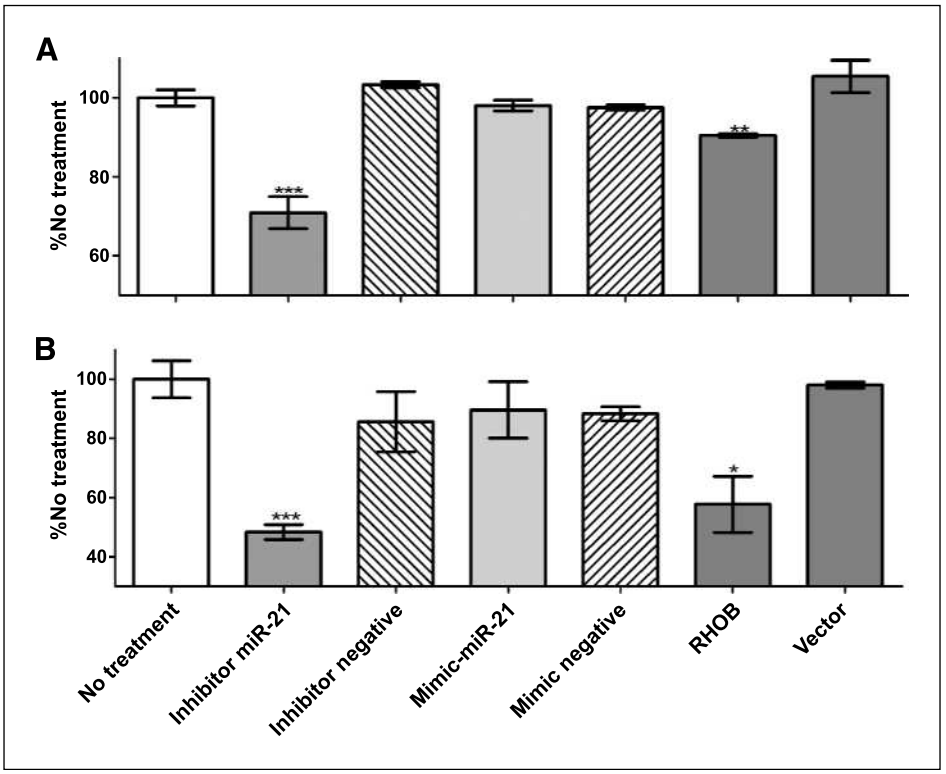

FIGURE 6. *In vitro* invasion assays were done in the Chemicon invasion chamber containing extracellular matrix. A, Huh-7 cells were incubated in the invasion chamber for 72 h. B, MDA-MB-231 cells were incubated in the invasion chamber for 24 h. The stained cells were eluted from membrane and absorbance at 560 nm was determined. Data are expressed as % no treatment (Lipofectamine only). *, $P < 0.05$; **, $P < 0.001$; ***, $P < 0.0001$.

versus untreated cells (33% wound closure; Fig. 2B, lane 15 versus lane 16).

miR-21 expression affects cell shape. To determine whether the loss of miR-21 affects cell shape, we visualized the actin cytoskeleton by phalloidin staining. Cell elongation was determined by measuring the ratio of the longest cord through the cell versus the longest axis perpendicular to it (24). In this assay, a reduction in the ratio reflects a "rounder," presumably less invasive, phenotype. All three cell lines treated with miR-21 inhibitor exhibited a switch to a significantly rounder phenotype by the assay (Fig. 5A and B; Supplementary Fig. S8). The rounded phenotype was most notably increased in the MDA-MB-231 cell line, which went from a ratio of 3.2 to 2.4 on knockdown of miR-21. The increase in rounded shape could be mimicked in the Huh-7 and MDA-MB-231 cell lines by direct overexpression of RHOB (Fig. 5C).

miR-21 expression promotes cell invasion. To determine whether miR-21 repression of RHOB affects cell invasion, an invasion chamber assay was used. In this assay, the ability of cells to invade through extracellular matrix is measured. HepG2, Huh-7, and MDA-MB-231 cells were transfected with miR-21 inhibitor, mimic, or RHOB expression vector and placed in an invasion chamber containing extracellular matrix. miR-21 inhibitor treatment decreased invasion of HepG2, Huh-7, and MDA-MB-231 cells by 10%, 29%, and 50%, respectively, compared with control inhibitor, which had no effect (Fig. 6A; Supplementary Fig. S9). In contrast, overexpression of RHOB in Huh-7 and MDA-MB-231 cells decreased invasion by 10% and 46%, respectively, as expected according to our working model. However, treatment with miR-21 mimic did not significantly increase the invasive abilities of the HCC cell lines (Fig. 6A and B; Supplementary Fig. S9).

Discussion

Metastasis is generally associated with poor prognosis and, in some cancers, increased miR-21 expression (6, 25, 26). Therefore, identifying the role of miR-21 in invasion and migration can have direct clinical implications. miRNA expression patterns indicate that miRNAs may play key roles in cancer development, yet the underlying mechanisms are largely unknown. The present study showed that overexpression of miR-21 increases MMP-9 activity in Huh-7, HepG2, and MDA-MB-231 cell lines. MMP expression is generally associated with invasive and/or metastatic phenotypes of tumors (19). We also showed that loss of miR-21 expression reduces migration and invasion *in vitro* in all three cancer cell lines. Furthermore, our miR-21 target analysis, for the first time, identified RHOB as a direct target of miR-21. We also confirmed a partial role for the tumor suppressor RECK, in conjunction with RHOB, in regulating the *in vitro* metastatic properties of our cell lines. This is consistent with earlier work that identified RECK as a tumor suppressor gene (27). In HCC, loss of RECK expression has been associated with poor prognostics (28).

The expression of RHOB is dramatically decreased as tumors become more aggressive (22, 29). In addition, RHOB has been shown to regulate cell shape, migration, and adhesion (30, 31). RHOB-null macrophage cells migrated faster than wild-type cells on fibronectin, which correlates with reduced adhesion, possibly due to a reduction in the integrin/RHOB signaling pathway and induction of cofilin (24).

miR-335 also acts as a tumor suppressor in a breast cancer cell line through the repression of migration and cell movement (32). Restoration of miR-335 expression in breast cancer cells led to a decrease in cell elongation (32). In contrast, this study identifies miR-21 as an oncogene that promotes the *in vitro* metastatic phenotypes of cell elongation, migration, and invasion by targeting the tumor suppressor RHOB. Knockdown of RHOB would be expected to cause destabilization of actin filaments needed for cell migration (33).

Furthermore, expression of miR-21 has a pro-proliferation and antiapoptotic function in HCC cell lines (11). This is also consistent with it targeting RHOB, which also has been shown to inhibit cell proliferation (22, 29). miR-21 causes antiapoptotic effects through the repression of such targets as PDCD4 (Asangani et al., 2008), PTEN, and BcL-2 (14, 16). In conclusion, the data in this report support a model in which miR-21 suppression of RHOB, in concert with RECK, contributes to increased ability of cells to metastasize. Understanding of miR-21 targets and pathways that this miRNA regulates could lead to new therapeutic strategies for a broad range of tumor types.

Disclosure of Potential Conflicts of Interest

No potential conflicts of interest were disclosed.

Grant Support

NIH grant CA37232 (C.E. Rogler), Pathobiology and Gene Therapy and Molecular Biology Research Cores of the Marion Bessin Liver Center grant 5P30DK41296, and Albert Einstein Comprehensive Cancer Center grant 5P30CA13330.

The costs of publication of this article were defrayed in part by the payment of page charges. This article must therefore be hereby marked *advertisement* in accordance with 18 U.S.C. Section 1734 solely to indicate this fact.

Received 10/23/2009; revised 03/26/2010; accepted 04/01/2010; published OnlineFirst 05/11/2010.

References

1. Gomaa AI, Khan SA, Toledano MB, Waked I, Taylor-Robinson SD. Hepatocellular carcinoma: epidemiology, risk factors and pathogenesis. World J Gastroenterol 2008;14:4300–8.
2. Mazzocca A, Liotta F, Carloni V. Tetraspanin CD81-regulated cell motility plays a critical role in intrahepatic metastasis of hepatocellular carcinoma. Gastroenterology 2008;135:244–56.
3. Morimoto O, Nagano H, Sakon M, et al. Diagnosis of intrahepatic metastasis and multicentric carcinogenesis by microsatellite loss of heterozygosity in patients with multiple and recurrent hepatocellular carcinomas. J Hepatol 2003;39:215–21.
4. Sakon M, Nagano H, Nakamori S, et al. Intrahepatic recurrences of hepatocellular carcinoma after hepatectomy: analysis based on tumor hemodynamics. Arch Surg 2002;137:94–9.
5. Bracken CP, Gregory PA, Khew-Goodall Y, Goodall GJ. The role of microRNAs in metastasis and epithelial-mesenchymal transition. Cell Mol Life Sci 2009;10:1682–99.
6. Medina PP, Slack FJ. microRNAs and cancer: an overview. Cell Cycle 2008;7:2485–92.
7. Ambros V, Chen X. The regulation of genes and genomes by small RNAs. Development 2007;134:1635–41.
8. Altuvia Y, Landgraf P, Lithwick G, et al. Clustering and conservation patterns of human microRNAs. Nucleic Acids Res 2005;33:2697–706.
9. Gabriely G, Wurdinger T, Kesari S, et al. MicroRNA 21 promotes glioma invasion by targeting matrix metalloproteinase regulators. Mol Cell Biol 2008;28:5369–80.
10. Zhu S, Wu H, Wu F, Nie D, Sheng S, Mo YY. MicroRNA-21 targets tumor suppressor genes in invasion and metastasis. Cell Res 2008;18:350–9.
11. Connolly E, Melegari M, Landgraf P, et al. Elevated expression of the miR-17-92 polycistron and miR-21 in hepadnavirus-associated hepatocellular carcinoma contributes to the malignant phenotype. Am J Pathol 2008;173:856–64.
12. Landgraf P, Rusu M, Sheridan R, et al. A mammalian microRNA expression atlas based on small RNA library sequencing. Cell 2007;129:1401–14.
13. Zhu S, Si ML, Wu H, Mo YY. MicroRNA-21 targets the tumor suppressor gene tropomyosin 1 (TPM1). J Biol Chem 2007;282:14328–36.
14. Si ML, Zhu S, Wu H, Lu Z, Wu F, Mo YY. miR-21-mediated tumor growth. Oncogene 2007;26:2799–803.
15. Meng F, Henson R, Wehbe-Janek H, Ghoshal K, Jacob ST, Patel T. MicroRNA-21 regulates expression of the PTEN tumor suppressor gene in human hepatocellular cancer. Gastroenterology 2007;133:647–58.
16. Papagiannakopoulos T, Shapiro A, Kosik KS. MicroRNA-21 targets a network of key tumor-suppressive pathways in glioblastoma cells. Cancer Res 2008;68:8164–72.
17. Liu AX, Rane N, Liu JP, Prendergast GC. RhoB is dispensable for mouse development, but it modifies susceptibility to tumor formation as well as cell adhesion and growth factor signaling in transformed cells. Mol Cell Biol 2001;21:6906–12.
18. Wang D, Dou K, Xiang H, et al. Involvement of RhoA in progression of human hepatocellular carcinoma. J Gastroenterol Hepatol 2007;22:1916–20.
19. Himelstein BP, Canete-Soler R, Bernhard EJ, Dilks DW, Muschel RJ. Metalloproteinases in tumor progression: the contribution of MMP-9. Invasion Metastasis 1994;14:246–58.
20. Chen Y, Liu W, Chao T, et al. MicroRNA-21 down-regulates the expression of tumor suppressor PDCD4 in human glioblastoma cell T98G. Cancer Lett 2008;272:197–205.
21. Oh J, Seo DW, Diaz T, et al. Tissue inhibitors of metalloproteinase 2 inhibits endothelial cell migration through increased expression of RECK. Cancer Res 2004;64:9062–9.
22. Mazieres J, Antonia T, Daste G, et al. Loss of RhoB expression in human lung cancer progression. Clin Cancer Res 2004;10:2742–50.
23. Kruger J, Rehmsmeier M. RNAhybrid: microRNA target prediction easy, fast and flexible. Nucleic Acids Res 2006;34:W451–4.
24. Wheeler AP, Ridley AJ. Why three Rho proteins? RhoA, RhoB, RhoC, and cell motility. Exp Cell Res 2004;301:43–9.
25. Zhang Z, Li Z, Gao C, et al. miR-21 plays a pivotal role in gastric cancer pathogenesis and progression. Lab Invest 2008;88:1358–66.

26. Qian B, Katsaros D, Lu L, et al. High miR-21 expression in breast cancer associated with poor disease-free survival in early stage disease and high TGF-β1. Breast Cancer Res Treat 2008;1:131–40.

27. Takahashi C, Sheng Z, Horan TP, et al. Regulation of matrix metalloproteinase-9 and inhibition of tumor invasion by the membrane-anchored glycoprotein RECK. Proc Natl Acad Sci U S A 1998;95: 13221–6.

28. Furumoto K, Arii S, Mori A, et al. RECK gene expression in hepatocellular carcinoma: correlation with invasion-related clinicopathological factors and its clinical significance. Hepatology 2001;33:189–95.

29. Huang M, Prendergast GC. RhoB in cancer suppression. Histol Histopathol 2006;21:213–8.

30. Tillement V, Lajoie-Mazenc I, Casanova A, et al. Phosphorylation of RhoB by CK1 impedes actin stress fiber organization and epidermal growth factor receptor stabilization. Exp Cell Res 2008;314:2811–21.

31. Taylor JM, Macklem MM, Parsons JT. Cytoskeletal changes induced by GRAF, the GTPase regulator associated with focal adhesion kinase, are mediated by Rho. J Cell Sci 1999;112:231–42.

32. Tavazoie SF, Alarcon C, Oskarsson T, et al. Endogenous human microRNAs that suppress breast cancer metastasis. Nature 2008;451: 147–52.

33. Lui WY, Lee WM, Cheng CY. Sertoli-germ cell adherens junction dynamics in the testis are regulated by RhoB GTPase via the ROCK/LIMK signaling pathway. Biol Reprod 2003;68:2189–206.